# Image and Conductivity Reconstruction of a Two-Dimensional Periodic Imperfect Conductor by the Genetic Algorithm

Wei Chien[1], Chi-Hsien Sun[2] and Ming-Hung Wu[3]*

[1]*Department of Electronic Engineering, De Lin Institute of Technology, Tucheng, Taiwan 236, R.O.C.*
[2]*Department of Electrical Engineering, Tamkang University, Tamsui, Taiwan 251, R.O.C.*
[3]*Department of Information Management, Cardinal Tien College of Healthcare & Management, Taipei, Taiwan 231, R.O.C.*

## Abstract

We consider the inverse problem of determining both the shape and the conductivity of a two-dimensional periodic conducting scatterer from knowledge of the far-field pattern of TM waves by solving the ill posed nonlinear equation. Based on the boundary condition and the measured scattered field, a set of nonlinear integral equations is derived and the imaging problem is reformulated into an optimization problem. The genetic algorithm is then employed to find out the global extreme solution of the object function. As a result, the shape and the conductivity of the conductor can be obtained. Numerical results are given to demonstrate that even in the presence of noise, good reconstruction has been obtained.

***Key Words***: Periodic Conducting Scatterer, Inverse Problem, Genetic Algorithm

## 1. Introduction

Due to the large area of applications such as non-destructive problems, geophysical prospecting and determination of underground tunnels and pipelines, etc, the inverse scattering problems related to the buried bodies are of particular importance in the scattering theory. In the past 20 years, many rigorous methods have been developed to solve the exact equations [1–9]. However, inverse problems of this type are difficult to solve because they are ill-posed and nonlinear [10]. As a result, many inverse problems are reformulated into optimization ones and then numerically solved by different iterative methods such as the Newton-Kantorovitch method [1–5], the Levenberg-Marquardt algorithm [6–8], and the successive-overrelaxation method [9]. Most of these approaches employ the gradient-based searching scheme to find the extreme of the cost function, which are highly dependent on the initial guess and usually get trapped in the local extreme. The genetic algorithm [11] is an evolutionary algorithm that uses the stochastic mechanism to search through the parameter space. As compared to the gradient-based searching techniques, the genetic algorithm is less prone to converge to a local extreme. This renders it an ideal candidate for global optimization. A few papers had applied the genetic algorithm to reconstruct the shape of a conductor [12–16]. However, to the best of our knowledge, there are still no numerical results by using the genetic algorithm for the periodic variable conducting scatterers. In this paper, we present a computational method to recover the shape of a periodic variable conducting cylinder based on the genetic algorithm. In section 2, the theoretical formulation for the inverse scattering is reported. The general principle of the genetic algorithms and the way we apply them are described. Numerical results are given for various objects

*Corresponding author. E-mail: mhwu@ctcn.edu.tw

of different shapes in section 3. Finally, some conclusions are drawn in section 4.

## 2. Theoretical Formulation

A periodic two-dimensional imperfectly conducting cylinder with conductivity $\sigma(\theta)$ is situated in a background medium with a permittivity $\varepsilon_o$ and a permeability $\mu_o$, as shown in Figure 1. The array is periodic in the x-direction with a periodic length $d$ and is uniform in the z-direction. The cross section of the metallic cylinder is assumed to be described in polar coordinates in xy plane by the equation $\rho = F(\theta)$. A plane wave whose electric field vector is parallel to the z-axis (i.e., transverse magnetic, or TM, polarization) is incident upon the periodic cylinder. Let $\vec{E}_i$ denote the incident wave with incident angel $\phi$, as shown in Figure 1. The scattered field, $\vec{E}_s = E_s \hat{z}$ can be expressed by

$$E_s(x,y) = \int_0^{2\pi} G_i(x,y;x',y') J(\theta') d\theta' \tag{1}$$

where

$$G_i(x,y;x',y') = \sum_{l=-\infty}^{\infty} \frac{1}{2\alpha_l d} \exp(-\alpha_l |y-y'|) \exp(-jk_l(x-x')) \tag{2}$$

$$J(\theta) = -j\omega\mu_0 \sqrt{F^2(\theta) + F'^2(\theta)}\, Js(\theta) \tag{3}$$

with

$$\alpha_l = \begin{cases} j\sqrt{k^2 - k_l^2}\,, & k^2 > k_l^2 \\ \sqrt{k_l^2 - k^2}\,, & k^2 \le k_l^2 \end{cases}, \quad k_l = \frac{2\pi l}{d} + k\sin\phi, \quad k^2 = \omega^2\varepsilon_0\mu_0 \tag{4}$$

Here $G_i(x, y; x', y')$ is the two-dimensional periodic Green's function [17,18], and $J_s(\theta)$ and $J(\theta)$ are the induced surface current density and an arc current density which is proportional to the normal derivative of electric field on the conductor surface, respectively. The boundary condition for a periodic imperfectly conducting scatterer with finite conductivity can be approximated by assuming that the total tangential electric field on the scatterer surface is related to surface current density through a surface impedance. This boundary condition yields an integral equation for $J(\theta)$:

$$E_i(F(\theta),\theta) = -\int_0^{2\pi} G_i(x,y;x',y') J(\theta') d\theta' + j\sqrt{\frac{j}{\omega\mu_0\sigma(\theta)}} \frac{J(\theta)}{\sqrt{F^2(\theta) + F'^2(\theta)}} \tag{5}$$

For the direct scattering problem, the scattered field $E_s$ is calculated by assuming that the periodic length $d$, the shape function $F(\theta)$ and the conductivity $\sigma(\theta)$ of the object are known. This can be achieved by first solving $J(\theta)$ in (5) and calculating $E_s$ in (1). For numerical calculation of the direct problem, the contour is first divided into sufficient small segments so that the induced surface current can be considered constant over each segment. Then the moment method is used to solve (5) and (1) with pulse basis function for expanding and Dirac delta function for testing. Note that, for numerical implementation of the periodic Green's function, we might face some difficulties in calculating this function. In fact, when $y$ approaches $y'$, the infinite series in (2) is very poor convergent. Fortunately, the infinite series may be rewritten as a rapidly convergent series plus an asymptotic series, which can be summed efficiently. Thus the infinite series in the periodic Green's function can be calculated efficiently [17,18].

Let us consider the following inverse problem: given the scattered field $E_s$ measured outside the scatterer, determine the shape $F(\theta)$ and the conductivity $\sigma(\theta)$ of the object. Assume the approximate center of the scatterer, which in fact can be any point inside the scatter, is known. Then the shape $F(\theta)$ function and conductivity function $\sigma(\theta)$ can be expanded as:

$$F(\theta) = \sum_{n=0}^{N/2} B_n \cos(n\theta) + \sum_{n=1}^{N/2} C_n \sin(n\theta) \tag{6}$$

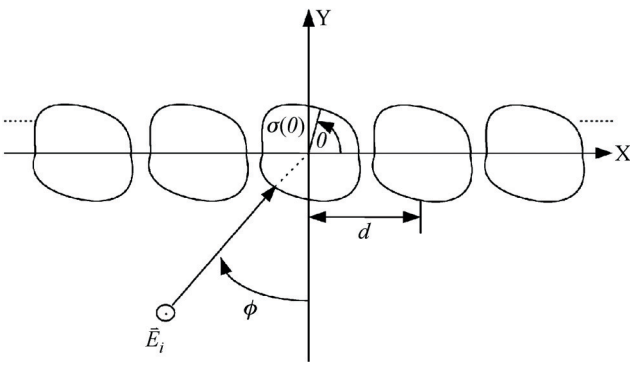


**Figure 1.** Geometry of a periodic imperfectly conducting cylinder with a periodic spacing $d$ along the x-direction.

$$\sigma(\theta) = \sum_{n=0}^{N/2} D_n \cos(n\theta) + \sum_{n=1}^{N/2} E_n \sin(n\theta) \tag{7}$$

where $B_n$, $C_n$, $D_n$ and $E_n$ are real coefficient to be determined, and $2 \times (N + 1)$ is the number of unknowns for shape function and conductivity function. In the inversion procedure, the genetic algorithm is used to minimize the following cost function:

$$CF = \{\frac{1}{M_t}\sum_{m=1}^{M_t}\left|E_s^{\exp}(\vec{r}_m) - E_s^{cal}(\vec{r}_m)\right|^2 / \left|E_s^{\exp}(\vec{r}_m)\right|^2 + \alpha\left|F'(\theta)\right|^2\}^{1/2} \tag{8}$$

where $M_t$ is the total number of measurement points. $E_s^{\exp}(\vec{r}_m)$ and $E_s^{cal}(\vec{r}_m)$ are the measured scattered field and calculated scattered field, respectively. Note that the regularization term $\alpha|F'(\theta)|^2$ was added in (8). Please refer the reference [4] for detail.

Genetic algorithms are the global numerical optimization methods based on genetic recombination and evolution in nature [19]. They use the iterative optimization procedures that start with a randomly selected population of potential solutions, and then gradually evolve toward a better solution through the application of the genetic operators: reproduction, crossover and mutation operators. In our problem, both parameters $B_n$ (or $C_n$, $D_n$ and $E_n$) are coded by the following equations:

$$B_n(C_n, D_n \text{ or } E_n) = p_{\min} + \frac{p_{\max} - p_{\min}}{2^L - 1}\sum_{i=0}^{L-1} b_i^{B_n(C_n, D_n \text{ or } E_n)} 2^i \tag{9}$$

The $b_0^{B_n(c_n, D_n \text{ or } E_n)}$, $b_1^{B_n(C_n, D_n \text{ or } E_n)}$, …, $b_{L-1}^{B_n(C_n, D_n \text{ or } E_n)}$ (gene) is the $L$-bit string of the binary representation of $B_n$ ($C_n$, $D_n$ or $E_n$), and $p_{\min}$ and $p_{\max}$ are the minimum and the maximum values admissible for $B_n$ ($C_n$, $D_n$ or $E_n$), respectively. Here, $p_{\min}$ and $p_{\max}$ can be determined by prior knowledge of the object. Also, the finite resolution with which $B_n$ ($C_n$, $D_n$ or $E_n$). The total unknown coefficients in (9) would then be described by a an $(N + 1) \times 2 \times L$ bit string (chromosome). The basic GA starts with a large population containing a total of $M$ candidates. A chromosome describes each candidate. Then the initial population can simply be created by taking $M$ random chromosomes. Finally, the GA iteratively generates a new population, which is derived from the previous population through the application of the reproduction, crossover, and mutation operators.

The new populations will contain increasingly better chromosomes and will eventually converge to an optimal population that consists of the optimal chromosomes. As soon as the object function (*OBF*) changes by < 1% in two successive generations and the number of generation exceeds pre-given one, the algorithm will be terminated and a solution is then obtained.

## 3. Numerical Results

By a numerical simulation, we illustrate the performance of the proposed inversion algorithm and its sensitivity to random error in the scattered field. Let us consider an imperfectly conducting cylinder array with a periodic length $d$ in free space and a plane wave of unit amplitude is incident upon the object, as shown in Figure 1. The frequency of the incident wave is chosen to be 3 GHz; i.e., the wavelength $\lambda$ is 0.1 m. In the examples, the size of the scatterer is about one third the wavelength, so the frequency is in the resonance range.

In our calculation, four examples are considered. To reconstruct the periodic length, the shape and the conductivity of the cylinder, the object is illuminated by two incident waves with incident angles $\phi = 45°$ and 135°, and the measurement points are taken on two lines with $Y = \pm 2$ m from x = -0.045 to 0.045 m. Each line has nine measurement points. Note that for each incident angle eighteen measurement points at equal spacing are used, and there are totally 36 measurement points in each simulation. The number of unknowns is set to 14, to save computing time. The population size is chosen as 250 (i.e., $M = 250$). The binary string length of the unknown coefficient, $B_n$ ($C_n$, $D_n$ or $E_n$) are also set to be 16 bits (i.e., $L = 16$). In other words, the bit number of a chromosome is 224 bits. The search range for the unknown periodic length is chosen from 0.05 to 0.1. The search range for the unknown coefficient of the shape function is chosen to be from 0 to 0.1 and the unknown coefficient of the conductivity is chosen to be from 1 to 200. The extreme value of the coefficient of the periodic length, the shape function and the conductivity can be determined by the prior knowledge of the objects. The crossover probability $p_c$ and mutation probability $p_m$ are set to be 0.8 and 0.04, respectively. The value of $\alpha$ is chosen to be 0.001.

In the first example, the shape and conductivity function are chosen to be $F(\theta) = (0.05 + 0.02 \cos \theta +$

0.015 sin 2θ) m with a periodic length $d = 0.2$ m and $\sigma(\theta) = (100 + 10\cos\theta + 10\cos 2\theta + 10\sin\theta + 10\sin 2\theta)$ S/m. The reconstructed shape function and conductivity function for the best population member (chromosome) are plotted in Figure 2(a) and Figure 2(b). Here DR and DSIG, which are called shape function and conductivity discrepancies respectively, are defined as

$$DR = \{\frac{1}{N'}\sum_{i=1}^{N'}[F^{cal}(\theta_i) - F(\theta_i)]^2 / F^2(\theta_i)\}^{1/2} \quad (10)$$

$$DSIG = \{\frac{1}{N'}\sum_{i=1}^{N'}[\sigma^{cal}(\theta_i) - \sigma(\theta_i)]^2 / \sigma^2(\theta_i)\}^{1/2} \quad (11)$$

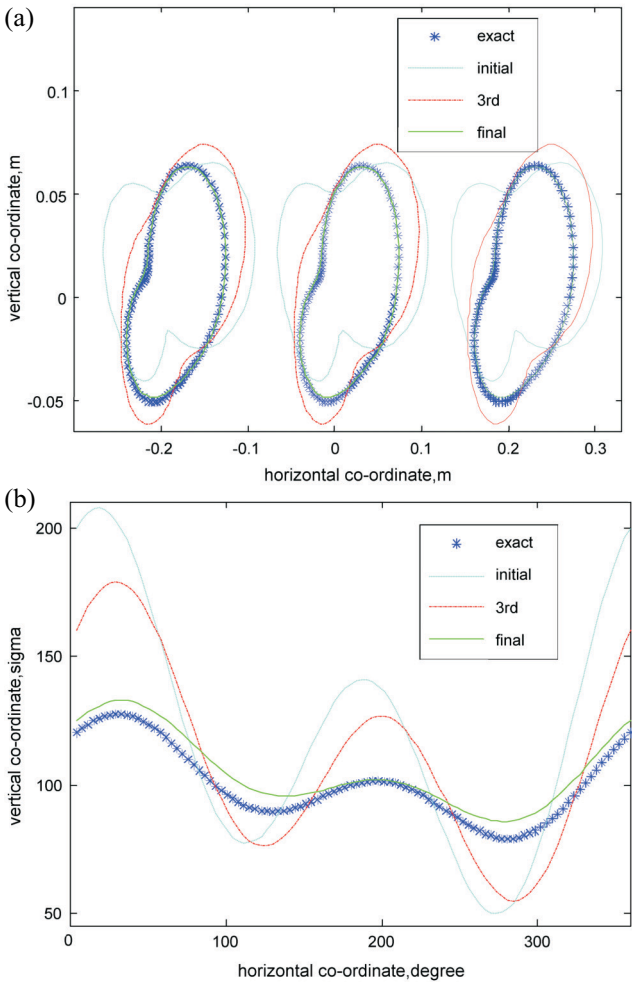


**Figure 2.** (a) Shape function for example 1. The star curve represents the exact shape, while the solid curves are calculated shape in iteration process. (b) Conductivity function for example 1. The star curve represents the exact conductivities, while the solid curves are calculated conductivities in iteration process.

where $N'$ is set to 100. Quantities *DR* and *DSIG* provide measures of how well $F^{cal}(\theta)$ approximates $F(\theta)$ and $\sigma^{cal}(\theta)$ approximates $\sigma(\theta)$, respectively. From Figure 2(a) and Figure 2(b), it is clear that the reconstruction of the shape and the conductivity function are quite good. In addition, we also see that the reconstruction of conductivity does not change rapidly toward the exact value until DR is small enough. This can be explained by the fact that the shape function makes a stronger contribution to the scattered field than the conductivity does. In other words, the reconstruction of the shape function has a higher priority than the reconstruction of the conductivity. To investigate the sensitivity of the imaging algorithm against random noise, two independent Gaussian noises with zero mean have been added to the real and imaginary parts of the simulated scattered fields. Normalized standard deviations of $10^{-5}$, $10^{-4}$, $10^{-3}$, $10^{-2}$ and $10^{-1}$ are used in the simulations. The normalized standard deviation mentioned earlier is defined as the standard deviation of the Gaussian noise divided by the rms value of the scattered fields. Here, the signal-to-noise ratio (SNR) is inversely proportional to the normalized standard deviation. The numerical result for this example is plotted in Figure 3. It is understood that the effect of noise is negligible for normalized standard deviations below $10^{-3}$.

In the second example, we select the following shape function $F(\theta) = (0.03 + 0.009\cos 3\theta)$ m and conductivity function $\sigma(\theta) = (80 + 15\cos 2\theta + 15\sin\theta + 20\sin 3\theta)$ S/m and a periodic length $d = 0.2$ m. The purpose of this example is to show that our method is able to reconstruct

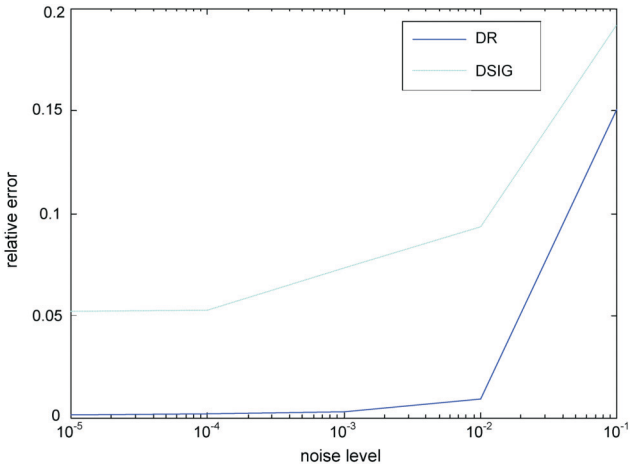


**Figure 3.** Relative error of shape and conductivity as a function of noise.

different shape conductivity. Satisfactory results are shown in Figure 4(a) and Figure 4(b).

In the third example, the shape and conductivity function are selected to be $F(\theta) = (0.05 + 0.02 \sin \theta + 0.01 \sin 2\theta + 0.01 \sin 3\theta)$ m and $\sigma(\theta) = (80 + 12 \cos \theta + 12 \sin 2\theta + 24 \sin 3\theta)$ S/m and a periodic length $d = 0.2$ m. Note that the shape function is not symmetrical about either x axis and y axis. This example has further verified the reliability of our algorithm. Refer to Figure 5(a) and Figure 5(b) for details.

## 4. Conclusion

We have presented a study of applying the genetic algorithm to reconstruct the shape and the conductivity of a periodic variable conducting cylinder through the knowledge of scattered field. Based on the boundary condition and the measured scattered field, we have derived a set of nonlinear integral equations and reformulated the imaging problem into an optimization one. By using the genetic algorithm, the shape and the conductivity of the object can be reconstructed. Even when the initial guess is far away from exact, the genetic algorithm converges to a global extreme of the object function, while the gradient-based methods often get stuck in a local extreme. Good reconstruction has been obtained from the scattered fields both with and without the addi-

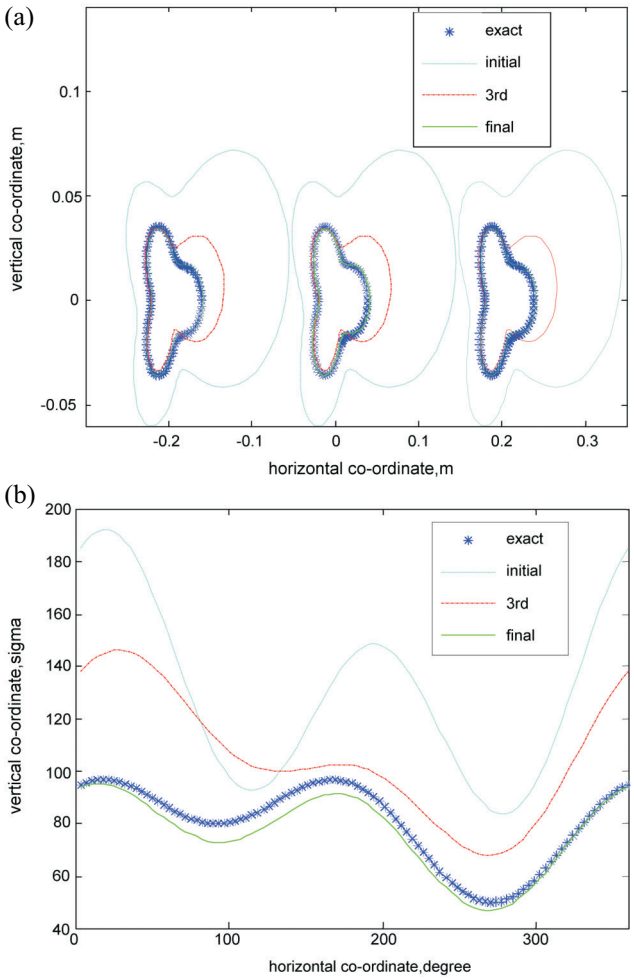


**Figure 4.** (a) Shape function for example 2. The star curve represents the exact shape, while the solid curves are calculated shape in iteration process. (b) Conductivity function for example 2. The star curve represents the exact conductivity, while the solid curves are calculated conductivities in iteration process.

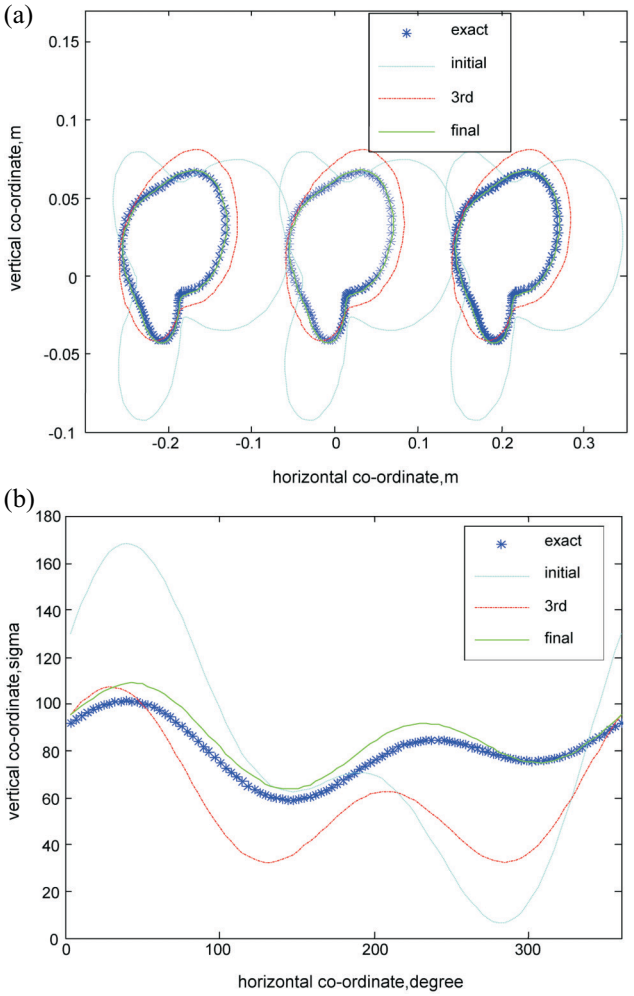


**Figure 5.** (a) Shape function for example 3. The star curve represents the exact shape, while the solid curves are calculated shape in iteration process. (b) Conductivity function for example 3. The star curve represents the exact conductivity, while the solid curves are calculated conductivities in iteration process.

tive Gaussian noise. According to our experience, the main difficulties in applying the genetic algorithm to this problem are how to choose the parameters, such as the population size ($M$), bit length of the string ($L$), crossover probability ($p_c$), and mutation probability ($p_m$). Different parameter sets will affect the speed of convergence as well as the computing time required. From the numerical simulation, it is concluded that a population size from 100 to 300, a string length from 8 to 16 bits, and $p_c$ and $p_m$ in the ranges of $0.7 < p_c < 0.9$ and $0.0005 < p_m < 0.05$ are suitable for imaging problems of this type.

## References


[1] Roger, A., "Newton-Kantorovitch Algorithm Applied to an Electromagnetic Inverse problem," *IEEE Trans. Antennas Propagat*., Vol. AP-29, pp. 232–238 (1981).

[2] Chiu, C. C. and Kiang, Y. W., "Inverse Scattering of a Buried Conducting Cylinder," *Inverse Problems*, Vol. 7, pp. 187–202 (1991).

[3] Chiu, C. C. and Kiang, Y. W., "Microwave Imaging of Multiple Conducting Cylinders," *IEEE Trans. Antennas Propagat*., Vol. 40, pp. 933–941 (1992).

[4] Otto, G. P. and Chew, W. C., "Microwave Inverse Scattering-Local Shape Function Imaging for Improved Resolution of Strong Scatterers." *IEEE Trans. Microwave Theory Tech*., Vol. 42, pp. 137–142 (1994).

[5] Kress, R, "A Newton Method in Inverse Obstacle Scattering Inverse Problem in Engineering Mechanics," ed. H. D. Bui et. al. (Rotterdam: Balkema), pp. 425–432 (1994).

[6] Colton, D. and Monk, P., "A Novel Method for Solving the Inverse Scattering Problem for Time-Harmonic Acoustic Waves in the Resonance Region II," *SIAM J. Appl. Math*., Vol. 46, pp. 506–523 (1986).

[7] Kirsch, A., Kress, R., Monk, P. and Zinn, A., "Two Methods for Solving the Inverse Acoustic Scattering Problem," *Inverse problems*, Vol. 4, pp. 749–770 (1998).

[8] Hettlich, F., "Two Methods for Solving an Inverse Conductive Scattering Problem," *Inverse Problems*, Vol. 10, pp. 375–385 (1994).

[9] Kleinman, R. E. and van den Berg, P. M., "Two-Dimensional Location and Shape Reconstruction," *Radio Sci*., Vol. 29, pp. 1157–1169 (1994).

[10] Hohage, T, "Iterative Methods in Inverse Obstacle Scattering: Regularization Theory of Linear and Nonlinear Exponentially Ill-Posed Problems," Dissertation Linz (1999).

[11] Goldgreg, D. E., *Genetic Algorithm in Search, Optimization and Machine Learning*, Addison-Wesley (1989).

[12] Chiu, C. C. and Liu, P. T., "Image Reconstruction of a Perfectly Conducting Cylinder by the Genetic Algorithm", *IEE Proc. Microw. Antennas Propag*., Vol. 143, pp. 249–253 (1996).

[13] Xiao, F. and Yabe, H., "Microwave Imaging of Perfectly Conducting Cylinders from Real Data by Micro Genetic Algorithm Couple with Deterministic Method", *IEICE Trans. Electron*., Vol. E81-C, pp. 1784–1792 (1998).

[14] Meng, Z. Q., Takenaka, T. and Tanaka, T., "Image Reconstruction of Two-Dimensional Impenetrable Objects Using Genetic Algorithm," *Journal of Electromagnetic Waves and Applications*, Vol. 13, pp. 95–118 (1999).

[15] Qian, Z., Ding, Z. and Hong, W., "Application of Genetic Algorithm and Boundary Element Method to Electromagnetic Imaging of Two-Dimensional Conducting Targets", *5th International Symposium on ISAPE*, pp. 211–214 (2000).

[16] Li, C. L., Chen, S. H., Yang, C. M., and Chiu, C. C., "Image Reconstruction for a Patially Immersed Perfectly Conducting Cylinder Using the Steady State Algorithm," *Radio Science*, Vol. 39, RS2016, April (2004).

[17] Jorgenson, R. E. and Mittra, R., "Efficient Calculation of Free-Space Periodic Green's Function," *IEEE Trans. Antenna Propagat*., Vol. 38, pp. 633–642 (1990).

[18] Wallinga, G. S., Rothwell, E. J., Chen, K. M. and Nyquist, D. P., "Efficient Computation of the Two-Dimensional Periodic Green's Function," *IEEE Tran. Antenna Propagat*., Vol. 47, pp. 895–897 (1999).

[19] Goldgerg, D. E., *Genetic Algorithm in Search, Optimization and Machine Learning*, Addison-Wesley (1989).


***Manuscript Received: Jan. 22, 2008***
***Accepted: Jul. 3, 2009***